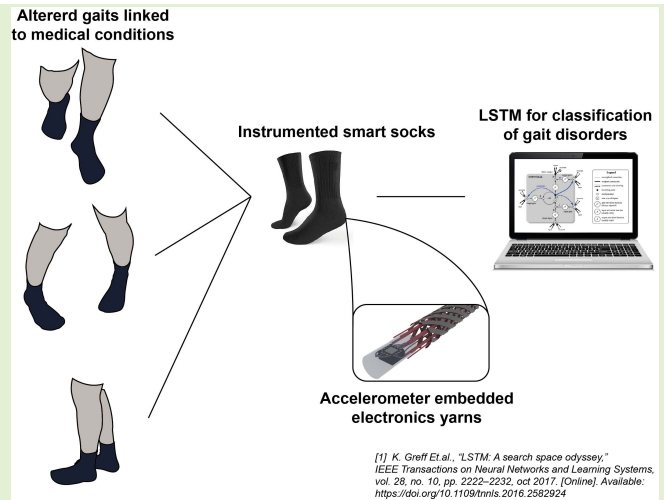


Classifying Gait Alterations Using an Instrumented Smart Sock and Deep Learning

Pasindu Lugoda¹, Fellow, IEEE, Stephen Clive Hayes¹, Theodore Hughes-Riley¹, Alexander Turner, Mariana V. Martins¹, Ashley Cook, Kaivalya Raval, Carlos Oliveira, Philip Breedon¹, and Tilak Dias

Abstract—This article presents a noninvasive method of classifying gait patterns associated with various movement disorders and/or neurological conditions, utilizing unobtrusive, instrumented socks and a deep-learning network. Seamless instrumented socks were fabricated using three accelerometer-embedded yarns, positioned at the toe (hallux), above the heel, and on the lateral malleolus. Human trials were conducted on 12 able-bodied participants, an instrumented sock was worn on each foot. Participants were asked to complete seven trials consisting of their typical gait and six different gait types that mimicked the typical movement patterns associated with various movement disorders and neurological conditions. Four neural networks and an SVM were tested to ascertain the most effective method of automatic data classification. The bi-long short-term memory (LSTM) generated the most accurate results and illustrates that the use of three accelerometers per foot increased classification accuracy compared to a single accelerometer per foot by 11.4%. When only a single accelerometer was utilized for classification, the ankle accelerometer generated the most accurate results in comparison to the other two. The network was able to correctly classify five different gait types: stomp (100%), shuffle (66.8%), diplegic (66.6%), hemiplegic (66.6%), and “normal walking” (58.0%). The network was incapable of correctly differentiating foot slap (21.2%) and steppage gait (4.8%). This work demonstrates that instrumented textile socks incorporating three accelerometer yarns were capable of generating sufficient data to allow a neural network to distinguish between specific gait patterns. This may enable clinicians and therapists to remotely classify gait alterations and observe changes in gait during rehabilitation.

Index Terms—Biomedical equipment, electronic textiles (E-textiles), gait monitoring, long short-term memory (LSTM), machine learning, sensors, smart textiles, wearable sensors.



Manuscript received 3 October 2022; accepted 17 October 2022. Date of publication 27 October 2022; date of current version 30 November 2022. This work was supported by the Engineering and Physical Sciences Research Council (EPSRC) through the “Production engineering research for the manufacture of novel electronically functional yarns for multifunctional smart textiles” under Grant EP/T001313/1. The associate editor coordinating the review of this article and approving it for publication was Prof. Xiaofeng Yuan. (Corresponding author: Pasindu Lugoda.)

This work involved human subjects or animals in its research. Approval of all ethical and experimental procedures and protocols was granted by the School of Science and Technology at Nottingham Trent University under Approval No. 1540613.

Pasindu Lugoda, Stephen Clive Hayes, Mariana V. Martins, Ashley Cook, Kaivalya Raval, and Philip Breedon are with the Department of Engineering, School of Science and Technology, Nottingham Trent University, NG11 8ET Nottingham, U.K. (e-mail: pasindu.lugoda@ntu.ac.uk; steve.hayes@ntu.ac.uk; mariana.venturamartins2020@my.ntu.ac.uk; ashley.cook2019@my.ntu.ac.uk; kaivalya.raval2019@my.ntu.ac.uk; philip.breedon@ntu.ac.uk).

Theodore Hughes-Riley, Carlos Oliveira, and Tilak Dias are with the Advanced Textiles Research Group, Nottingham School of Art and Design, Nottingham Trent University, NG1 4GG Nottingham, U.K. (e-mail: theo.hughes-riley@ntu.ac.uk; jose.oliveira@ntu.ac.uk; tilak.dias@ntu.ac.uk).

Alexander Turner is with the Department of Computer Science, University of Nottingham, NG8 1BB Nottingham, U.K. (e-mail: alexander.turner@nottingham.ac.uk).

Digital Object Identifier 10.1109/JSEN.2022.3216459

This work is licensed under a Creative Commons Attribution 4.0 License. For more information, see <https://creativecommons.org/licenses/by/4.0/>

I. INTRODUCTION

THE ability for wearable textile devices to be worn comfortably, in close proximity to the human body, makes them potent candidates for continuous monitoring of physiological parameters [1], [2], [3], [4]. For this reason, numerous wearable electronic textile (E-textile) sensors have been generated and used to monitor various parameters, including temperature [5], sweat production [6], heart rate [7], and strain [8], [9], [10]. The capacity of this type of data collection to facilitate the diagnosis and monitoring of different medical conditions provides opportunities to improve patient care and rehabilitation outcomes [11], [12], [13], [14], [15]. Since the primary method of human locomotion is walking, it is one of the most studied human movements [16], [17], [18], [19], [20], and it can be used as a predictor of morbidity and mortality [19], [20], as well as having implications on activities of daily living. In particular, rehabilitation of gait in individuals with Parkinson’s disease, stroke, head injury, diabetic neuropathy, multiple sclerosis, cerebral palsy, brain lesions, and spinal cord injuries can be a determinant of an individual’s capacity to return to an independent life [21], [22], [23], [24], [25], [26], [27], [28].

To create effective personalized gait rehabilitation interventions, clinicians and therapists must have evidence-based methods of analyzing gait [29]. The current “gold standard” for gait analysis takes place in a laboratory setting, often within a constrained room or space [30]. A popular method of analyzing and recognizing gait abnormalities uses 3-D motion capture camera systems [31], [32], [33], [34], [35], [36]. Additional technologies utilized include force plates, instrumented walkways, instrumented treadmills, EMG systems, and movable footplates, all of which can be integrated with motion capture technology [13], [37], [38], [39], [40], [41]. Typically, the use of these systems limits the user’s movements to a certain area. Furthermore, these systems are often used in combination adding to the distress of the patient and complicating the data-processing procedures for the clinician [42]. The use of these combined systems is extremely costly and requires a trained operator. This type of monitoring also limits the capacity of the clinician to monitor gait over a prolonged period, limiting the opportunity to view the impacts of fatigue [43].

A proposed solution to the aforementioned problems is to use a wearable device to continuously monitor gait. Numerous wearable devices have been created for this purpose [44], [45]. The capacity of such sensors to collect continuous data without requiring expensive laboratory equipment and dedicated laboratories has led to a boom in the development of such equipment [15]. While many wearable systems have been developed, there are still limitations. In some systems, the electronics can obstruct the free movement of the user, leading to adverse effects on movement quality, negatively impacting the ability to record the individual’s typical movement patterns, resulting in deleterious consequences for rehabilitation [46], [47]. Shoes, socks, and insoles have been the preferred wearable options for gait analysis due to their unobtrusive nature [37], [48], [49], [50], [51], [52], [53], [54], [55], [56], [57], [58], [59], [60], [61], [62], [63]. Of these devices most have utilized pressure sensors to monitor gait [37], [48], [49], [51], [52], [53], [54], [55], [56], [57], [58], [59], [60], [63]. In general, pressure sensors can be affected by hysteresis leading to poor reliability [64]. Fiber-optic-based pressure-sensing systems are less prone to hysteresis; however, these can be easily damaged when walking [64]. As an alternative, some researchers have utilized accelerometers [50], [60], [62] and inertial measurement units [49], [61] for gait analysis. The majority of these devices are large/bulky and have not been seamlessly integrated into the wearable garment, adversely impacting the comfort of the wearer and impeding movement [60], [61], [62]. The use of IMUs and accelerometers has typically only generated data from a single point located on the foot (based on a single sensor), which may not provide sufficient data to classify gait alterations [61], [62].

E-textile-based “smart socks” are one such product that has been developed to track gait outside of the laboratory [53], [54], [55], [56], [57], [58], [59], [60], [63]. Numerous versions have been designed using pressure sensors, either attached to the surface of the sock [58], [59], [60], [63] or that utilize textile-based pressure sensors [53], [54], [55], [56],

[57]. Surface-based sensors on the socks are likely to be affected by abrasion, whereas textile-based pressure sensors are characteristically adversely affected by hysteresis [64], [65], [66], [67]. The majority of sock systems still use pressure sensors and have focused on identifying heel strike and toe-off, allowing easy identification of temporal–spatial gait parameters but limiting their ability to distinguish between gait types. Alternative devices have been developed that can distinguish between the gait patterns of different individuals and identify various human activities such as running, leaping, and sliding [63]. Each of these activities generates a significantly different movement pattern from each of the others. Consequently, the ability of this type of device to capture subtle changes in motion, such as differences in gait patterns, has not been assessed.

Each of these approaches, especially when used to continuously monitor gait over a prolonged period, generates vast amounts of data. This alone makes the already challenging task of analyzing movement even more difficult. The use of machine learning to automate the processing and analysis of large volumes of gait data has become more common in recent years. Researchers have classified gait abnormalities using shallow machine-learning tools such as random forest, K nearest neighbor, and support vector machine-learning tools [42], [50], deep neural networks such as long short-term memory (LSTM) networks [52], [68] and convolutional neural networks (CNN) [69]. The use of these tools to identify gait features has typically been more successful with multisensor and even multimodality data collection [42]. These data have generally been collected using wearables that were not based on smart textiles [50], [52], [70]. For some of these devices, the electronics have not been seamlessly integrated into wearable systems.

To overcome the limitations identified in the literature, a pair of socks was instrumented with six yarn-embedded triaxial accelerometers (three per sock). By embedding the electronics within the structure of a yarn (creating an electronic yarn or E-yarn), the esthetics and feel of the garment were maintained. The core technology to create E-yarns has previously been used to generate temperature sensing [71], [72], acoustic sensing [73], and solar energy harvesting yarns [74]. Accelerometry-based E-yarns have been used within vibration sensing gloves [75]. The aim of the current work was to use a deep-learning neural network to automatically classify gait differences noninvasively, based on multisensor data from a pair of instrumented smart socks created using E-textiles. The dataset used in this work was distinctive to this research and represents the first time data collected from a wearable system has been utilized to classify seven different gait patterns associated with various movement disorders and/or neurological conditions. The data from the instrumented sock was analyzed using three types of neural networks and a support vector machine (SVM) classifier in order to identify the best-performing neural network. It was hypothesized that: 1) the multisensor data (provided by three sensors for each foot) would generate a better classification accuracy than a single accelerometer per foot and 2) that the neural network

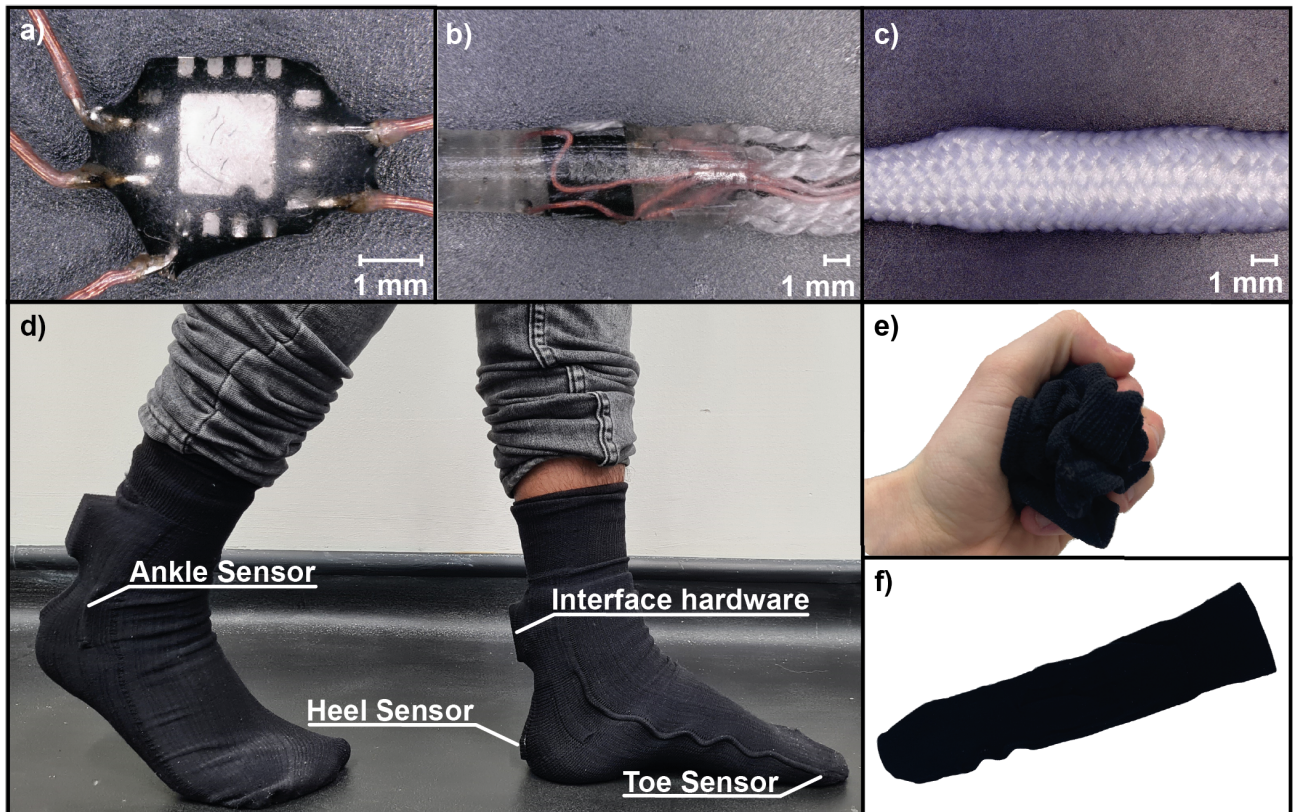


Fig. 1. Instrumented smart sock and the electronic yarn fabrication process. (a) ADXL337 accelerometer soldered onto the flexible Litz wires. (b) Polymer resin micropod around the soldered accelerometer and supporting yarns. (c) Accelerometer-embedded electronic yarn: encapsulated accelerometer, Litz wires, and supporting yarns. (d) Accelerometer locations on the instrumented sock, lateral malleolus, posterior calcaneus, and medial to the hallux. (e) Ability of the sock to undergo textile deformations. (f) Inside of the sock demonstrating lack of visible E-yarns.

would be able to accurately classify each of the gait profiles generated in the data collected based on distinctive time-series data.

II. MATERIALS AND METHODS

A. Fabrication of the Instrumented Smart Sock

The accelerometer-embedded E-yarns were constructed in three stages. Initially, a triaxial, analog accelerometer with a sensitivity of 300 mV/g (microelectrochemical systems, ADXL337, Analog Devices, Norwood, MA, USA) was soldered onto five flexible Litz wires. Each Litz wire consisted of seven enameled copper strands, covered in a nylon sheath with a diameter of 254 μm (BXL2001, OSCO Ltd., Milton Keynes, U.K.). This created five solder discrete joints corresponding to the axis outputs (x -axis, y -axis, and z -axis), the voltage input, and the ground [see Fig. 1(a)]. The soldered accelerometer was then encapsulated within a resin micropod (Dymax 9001-E-V3.7; Dymax, Corporation, Torrington, CT, USA). The micropod included eight textured, multifilament, polyester yarns, 36 filaments/167 dtex (Ashworth and Sons, Cheshire, U.K.) that ran parallel to the copper wires and provided additional mechanical support to the yarns [see Fig. 1(b)]. The final accelerometer-embedded E-yarn was created by inserting the encapsulated accelerometer, Litz wires, and supporting fibers into a suture braider (RU1/24-80; Herzog GmbH, Oldenburg, Germany). The covering braided structure consisted of 24 carriers with polyester yarns, 36 filaments/167 dtex

(Ashworth and Sons, Cheshire, U.K.) and a lay length of 5 was used [see Fig. 1(c)].

A seamless knit sock was subsequently produced using a Stoll ADF 3 flatbed knitting machine. The sock was knit with integrated channels for the insertion of the accelerometer yarns and a pocket to accommodate the interface electronics. The sock comprised of three types of yarns, a single cover lycra 16/SCY/090 with a nylon 6.6 covering (Stretchline, Long Eaton, U.K.), a two yarn 20/DCY/003 nylon 6.6, and a 1/78/68 Nylon 6.6 yarn (ContiFibre, Casaloldo, Italy). Once fabricated, three accelerometer yarns were inserted into the sock and stitched in place. These yarns were positioned approximately over the lateral malleolus, posterior to the calcaneus, and medially to the hallux [see Fig. 1(d)]. The integrated electronics did not impact on the textile's flexibility or deformability [see Fig. 1(e)]. To ensure that the electronics would not lead to skin damage in participants and patients, the sock was designed to ensure no presence of the electronics was evident inside the sock as evidenced in Fig. 1(f). The interface electronics used to capture the data and power the accelerometers consisted of a Teensy LC (PJRC, Oregon, USA) microcontroller wired to the analog input of each accelerometer. The ensemble was housed within a 3-D printed thermoplastic polyurethane casing. This was inserted into the knit pocket of the sock. The Teensy boards were connected to a computer using USB cables throughout the experiments, however, the hardware solution could be

made wireless in future iterations. Python (Python Software Foundation, Delaware, USA) was utilized to capture the data from the two microcontrollers.

B. Testing the Instrumented Smart Sock

1) *Participants*: 12 able-bodied injury-free individuals: five males and seven females, aged 22–42 years, mass 58–97 kg, U.K. shoe size 4–8.5, were recruited for this study. Ethical approval was granted by the noninvasive ethics committee for the School of Science and Technology at Nottingham Trent University (approval number 1540613). All participants gave written informed consent before testing.

2) *Protocol*: Participants were asked to walk around a figure of eight walkways (30.6 ± 0.12 m in length) for 180 s per trial wearing a pair of the instrumented smart socks. The seven experimental conditions consisted of distinct gait features associated with specific neurological and physical conditions. Table I presents the gait features of each experimental condition and its associated medical condition. All participants were provided with a pair of instrumented smart socks to wear and were instructed on how to wear the socks to ensure the accelerometers were positioned in the correct locations. Before each experimental walking condition, the participant was shown the walking pattern they were required to mimic and was given time to practice the pattern ensuring they could replicate the appropriate movement characteristics. When data capture was ready to begin, the participants were given simple instructions; on the command “Go,” they would walk around the figure of eight track (marked out on the laboratory floor), using the specific gait pattern they had been shown until they were told to stop by the researcher. After each trial was complete, the participant was given time to rest if needed and the next gait pattern was demonstrated. Once the participant had experienced sufficient rest (minimum of 2 min) they were asked to practice the new gait pattern before data collection. This process was repeated until all experimental conditions were complete. The order in which each participant was asked to complete the walking trials was randomized to remove the impact of fatigue when walking using an unfamiliar gait pattern.

Once the data were recorded, each file was labeled and assigned to a specific folder based on the gait pattern being mimicked. Triaxial acceleration data were recorded at 87.5 Hz generating 141 687 data points per foot, per trial. The vectors generated were combined into 2-s data instances consisting of data from all three accelerometers from both socks. Approximately 75% of the data captured was provided to the neural networks for training purposes and the remaining 25% of the data was split evenly between the testing and validation sets. This split represents the entirety of nine participants’ data being used for training, and the remaining three participants (5, 6, 7) data being used for testing and validation. The process of restricting 25% of the data for testing enables evaluation of each neural network trained using unseen data, providing information about the capacity of each network to classify new data (not used in the training process). As well as accuracy measures, precision, recall, and specificity were calculated for each neural network as well as time performance. Each

TABLE I
DIFFERENT GAIT TYPES EVALUATED USING THE SOCK

Gait type	Description	Associated medical condition
Normal gait	Smooth, continuous ambulation with minimal effort	N/A
Hemiplegic or hemipastic gait	Initial toe contact on hemiparetic side, mechanically induced increased limb length in swing due to reduced hip and knee flexion and ankle plantar flexion resulting in toe dragging or hip circumduction [28], [77]	Stroke, head injury, Cerebral palsy
Steppage gait	Weakness of the dorsiflexor muscles resulting in drop foot and an equinus position of the ankle. The foot hangs in plantar flexion leading to reduced toe clearance, as a compensation hip and knee flexion in swing is increased and the initial contact often occurs with a flat or forefoot contact altering the typical foot progression throughout stance [27], [78]	Equinus contractures, stroke, pelvic or spinal trauma
Shuffling or Parkinsonian gait	Reduced hip extension, knee extension and ankle plantar flexion throughout pre-swing and initial swing phases. Results in short “shuffling steps” with soles of feet barely leaving the floor [28], [79]	Parkinson’s Disease and PAD-IC (Peripheral arterial disease – intermittent claudication)
Diplegic gait	Bilateral spasticity of the adductors and hip flexors, extension of the knees and plantar flexion of the ankles, leads to bilateral circumduction of the legs which can lead to a “scissoring” like action with the feet crossing over [27], [28]	Bilateral spasticity, Cerebral palsy, cervical spondylotic myelopathy, and multiple sclerosis
Foot slap	Weakness or total/partial paralysis of the muscles controlled by the peroneal nerve (pretibial muscles I.e., tibialis anterior). After initial heel contact the forefoot rapidly drops to the ground generating a slap sound [80]	Multiple sclerosis, spinal disorders
Stomping or sensory ataxic gait	Insufficient sensory information is available for the individual to know where their foot is in relation to the ground in terms of distance and position/angle (neurological/visual/proprioceptive). A stomping action is used to ensure firm contact. This is accompanied by a wide step width and short step length [26]	Diabetic neuropathy

instance of data was generated with a 50-time-step gap (sampled at 87.5 Hz) between itself and its predecessor to ensure comprehensive sampling of the data without introducing prohibitive time costs for the training of the neural networks. The neural networks were optimized using the adaptive moment estimation optimizer with a minibatch size of 128. The training was automatically stopped after the validation set showed 20 consecutive steps with lower accuracy than the current best. At this point, the current best network was returned and the training stopped. The network was then evaluated using the test data.

C. Neural Network Structures Utilized for Classification of the Data

LSTMs are a type of recurrent neural network [80] which have shown significant promise in the classification of time series data in a range of fields [52], [68], [81] and have been applied in the medical industry to better understand

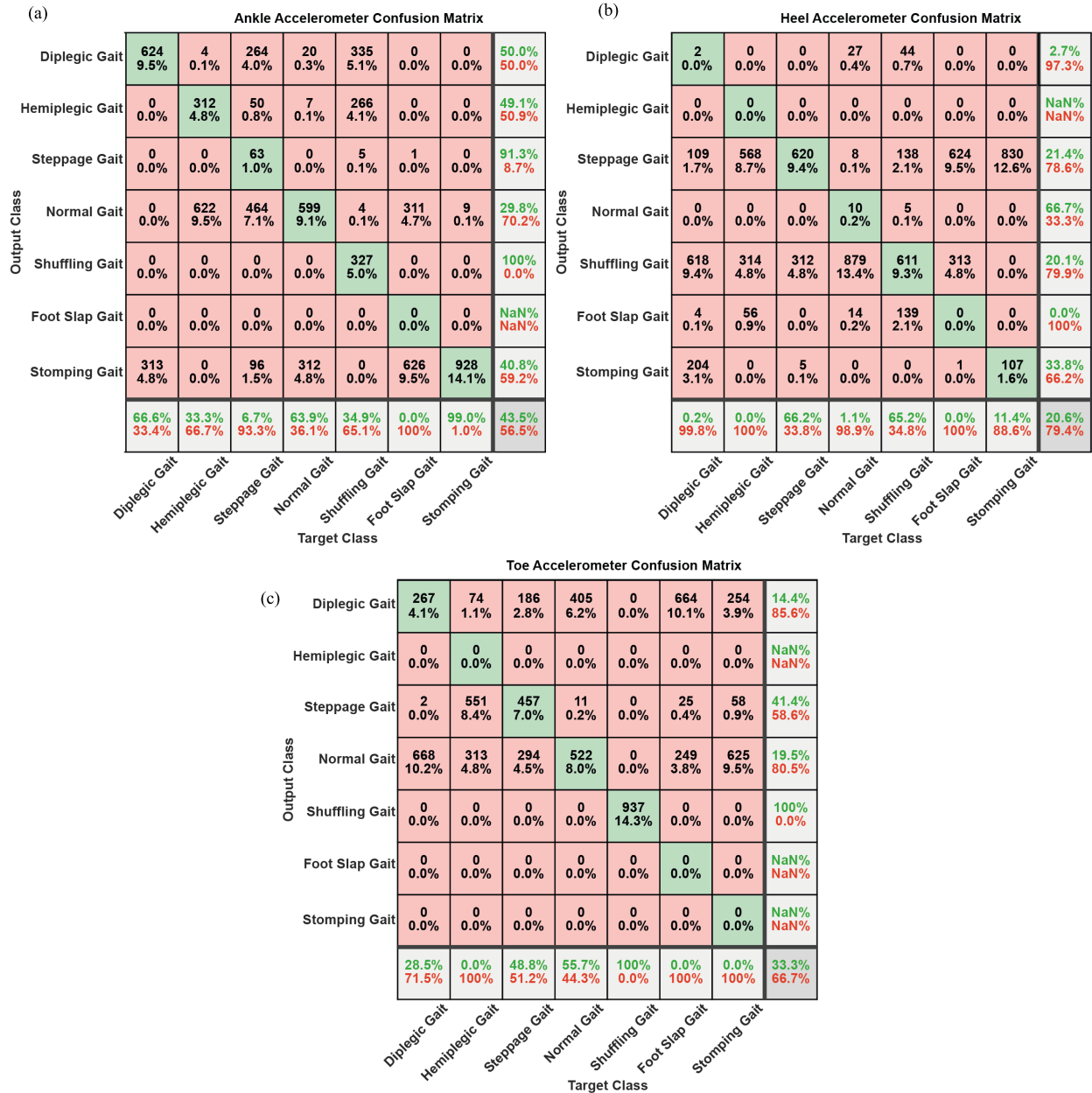


Fig. 2. Confusion matrices illustrating the results for the most accurate network for each of the single accelerometers when classifying the various gait types. (a) Ankle located accelerometer (overall accuracy 43.8%). (b) Heel located accelerometer (overall accuracy 20.6%). (c) Toe located accelerometer (overall accuracy 33.3%).

movements in a variety of contexts. LSTMs can learn features and representations within data over both long and short periods of time. Bi-LSTMs, which were used in this work, are a particular type of LSTM where the input flows in both directions rather than unidirectionally within the LSTM. This has resulted in better performance for a range of tasks [52], [82]. The Bi-LSTMs used in this work contained 200 cells that were shaped according to seven layers: sequence input, Bi-LSTM, dropout, RELU layer fully connected, SoftMax, and classification layers. The information depicting this can be seen in Table II.

To ascertain the suitability of the Bi-LSTM in the context of this work, the data was applied to three other neural network architectures and an SVM classifier. The three architectures were a CNN, a Bi-LSTM CNN (Bi-LSTM-CNN), and an

TABLE II
ILLUSTRATION OF THE BI-LSTM MODELS, DEPICTING THE INDIVIDUAL LAYERS, USED TO CLASSIFY THE DATA IN THIS WORK

Bi-LSTM Topology
Sequence Input Layer
Dropout Layer (0.5)
Bi-LSTM Layer (200 units)
Dropout Layer (0.5)
ReLU Layer
Fully Connected Layer
Softmax Layer
Output Layer

LSTM network. All of the networks and the SVM were trained using the same data as the Bi-LSTM in this work. Broadly, the Bi-LSTM was found to outperform the three

other three networks tested, with the Bi-LSTM CNN and LSTM marginally behind. The CNN and the SVM performed markedly worse and were generally unable to learn the features within the data. The full results of these experiments, along with the topologies of the networks, can be found in Table III in the Appendix.

III. RESULTS AND DISCUSSION

Four neural networks and an SVM classifier were tested to identify the most appropriate method for use with the dataset generated by the smart socks, the results of which can be found in Fig. 4 in the Appendix. The CNN was only able to achieve a classification percentage just above random (100/7 classes = 14.2%). Similarly, the SVM produced a classifier similar to random choice. The Bi-LSTM-CNN performed well, achieving a 53.4% accuracy, which was slightly worse than the Bi-LSTM, however, short shuffling gait and diplegic gait were both correctly classified more than 70% of the time, whereas no other gait type was classified correctly more than 60% of the time. Finally, the LSTM produced a classification of 52.7%, although no trials were classified as high stepping gait (even in error) and slap foot gait was never correctly classified and a total of ten normal gait trials were misclassified as slap foot by the network. It is worth noting that due to the shape of the input data, it was only possible to generate convolutions of small size; in experiments with “bigger data,” it is possible that the CNNs would present a more promising result. Consequently, the Bi-LSTM is presented in most detail within the method section, as it performed best out of all the networks trialed.

The primary aim of this work was to combine an instrumented smart sock and a neural network to classify different gait profiles. It was hypothesized that the multisensor data (provided by three sensors for each foot) would generate a better classification accuracy than a single accelerometer per foot. The results obtained when a single accelerometer yarn was used for the classification of gait are presented in Fig. 2(a)–(c). The accelerometer located on the ankle produced the highest overall accuracy compared to the other two locations. An accuracy of 43.5% [see Fig. 2(a)] was observed for the accelerometer located on the ankle. The Bi-LSTM was able to classify stomp gait 99.0% of the time when only the ankle accelerometer was used. Nonetheless, this gait was overclassified by the network and only 40.8% of the total data identified as stomp gait was actually data corresponding to this gait. As shown in Fig. 2(b), the lowest overall accuracy of 20.6% was demonstrated when only data from the heel accelerometer was used. The heel accelerometer correctly identified steppage gait 66.2% of the time. Data from the toe accelerometer produced an overall accuracy of 33.3% as illustrated in Fig. 2(c). Although it generated a low overall classification accuracy, shuffling gait showcased a classification accuracy of 100%. The overall classification accuracy for the smart sock with all accelerometry data provided for the Bi-LSTM was 54.9% (see Fig. 3). Previous work has suggested that data from multiple sensors increases the capacity for neural networks to correctly classify gait features [42]. The data presented here concurs with this statement, showing that the use of multiple sets of

Output Class	Diplegic Gait	Hemiplegic Gait	Steppage Gait	Normal Gait	Shuffling Gait	Foot Slap Gait	Stomping Gait	
Diplegic Gait	624 9.5%	0 0.0%	109 1.7%	0 0.0%	292 4.4%	1 0.0%	0 0.0%	60.8% 39.2%
Hemiplegic Gait	0 0.0%	625 9.5%	0 0.0%	313 4.8%	0 0.0%	0 0.0%	0 0.0%	66.6% 33.4%
Steppage Gait	0 0.0%	0 0.0%	45 0.7%	0 0.0%	18 0.3%	114 1.7%	0 0.0%	25.4% 74.6%
Normal Gait	0 0.0%	309 4.7%	229 3.5%	544 8.3%	0 0.0%	15 0.2%	0 0.0%	49.6% 50.4%
Shuffling Gait	255 3.9%	0 0.0%	0 0.0%	0 0.0%	626 9.5%	46 0.7%	0 0.0%	67.5% 32.5%
Foot Slap Gait	0 0.0%	4 0.1%	0 0.0%	0 0.0%	1 0.0%	199 3.0%	0 0.0%	97.5% 2.5%
Stomping Gait	58 0.9%	0 0.0%	554 8.4%	81 1.2%	0 0.0%	563 8.6%	937 14.3%	42.7% 57.3%
	66.6% 33.4%	66.6% 33.4%	4.8% 95.2%	58.0% 42.0%	66.8% 33.2%	21.2% 78.8%	100% 0.0%	54.9% 45.1%
	Diplegic Gait	Hemiplegic Gait	Steppage Gait	Normal Gait	Shuffling Gait	Foot Slap Gait	Stomping Gait	

Fig. 3. Confusion matrix presenting output and classification accuracy for the best-performing network based on data from all three accelerometers from each sock. Overall classification accuracy for the network was 54.9%.

sensor data improved the classification accuracy of the network by over 11%.

The second hypothesis was that the Bi-LSTM would be able to accurately classify each of the gait profiles. The Bi-LSTM in combination with the instrumented smart socks allowed for the correct classification of five of the seven gait profiles (see Fig. 3). The results demonstrate that stomping gait was correctly classified 100% of the time. However, the network also misclassified other gaits as stomping gait. It can be observed that 57.3% of the time, other gait types were misclassified as stomp gait. This was plausible because stomping generated the highest acceleration values through the rapid change of acceleration in the vertical and anterior–posterior directions associated with large ground impacts [26]. Since other gait types also had phases of high acceleration, this may have limited the network’s capacity to classify the gait type based on feature differences. The short shuffling gait was identified with the next best accuracy of 66.8% closely followed by the diplegic and hemiplegic gait classifications (66.6%). Although both the short shuffling and diplegic gait profiles were correctly classified over 66% of the time, they were both misclassified as each other, more than as any other gait type. This was most likely due to the short shuffling gait generating minimal acceleration compared to the other gait profiles as the foot only leaves the floor by a small distance [78]. During diplegic gait, most participants walked very slowly due to it being a difficult gait to perform, this may have resulted in the acceleration profiles of both shuffling and diplegic gait being quite similar.

Hemiplegic and normal gait were also misclassified as each other, even though they were correctly classified by the network most of the time, 66.6% and 58.0%, respectively. Hemiplegic gait has an asymmetrical profile where one of

TABLE III

ILLUSTRATIONS OF THE BI-LSTM CONVOLUTIONAL NEURAL NETWORK, CONVOLUTIONAL NEURAL NETWORK, AND LSTM NETWORK, DEPICTING THE INDIVIDUAL LAYERS, USED TO CLASSIFY THE DATA IN THIS WORK

Network Topology		
Bi-LSTM-CNN	Convolutional Neural Network	LSTM
Sequence Input Layer	Sequence Input Layer	Sequence Input Layer
Dropout Layer	Dropout Layer	Dropout Layer
1x1 Convolutional Layer	1x1 Convolutional Layer	LSTM layer (200 units)
Bi-LSTM layer (200 units)	ReLU Layer	Dropout Layer
Dropout Layer	MaxPooling layer	ReLU Layer
Flatten Layer	Fully Connected Layer	Fully Connected Layer
ReLU Layer	Softmax Layer	Softmax Layer
Fully Connected Layer	Output Layer	Output Layer
Softmax Layer		
Output Layer		

the legs performs the expected “normal” movement, while the other leg circumducts to compensate for the inability to flex the knee [76]. Although there is an asymmetrical distribution of the gait parameters, the change in acceleration may not have been sufficient to identify it as asymmetrical. Additionally, there is still a heel strike and controlled shift of weight from one leg to the other. Moreover, this condition was easier for participants to replicate than most of the other gait profiles, allowing them to walk at a more natural speed which again may have been a factor associated with the Bi-LSTM confusing hemiplegic gait and normal walking.

Both the foot slap and steppage gait were misclassified more often than they were correctly identified by the Bi-LSTM (21.2% and 4.8%, respectively). These two gaits were most often misclassified as stomping gait (60.1% foot slap gait data and 58.7% steppage gait data). In foot slap gait, the high acceleration recorded by the toe accelerometer as the forefoot rapidly drops to the ground may have confused the network into classifying it as stomping gait [79]. Steppage gait requires the foot to be lifted higher, and this exaggerated foot movement might have caused an increase in acceleration, causing the algorithm to misclassify it as stomping gait [27], [77]. Foot slap gait was incorrectly classified as steppage gait 11.9% (114 times out of a possible 938 instances). However, steppage gait was never misclassified as foot slap gait. This suggests that the Bi-LSTM was able to distinguish steppage gait from foot slap gait even though it was incapable of distinguishing it from the other gait conditions. This is probably due to the foot slap gait generating a heel initial contact rather than mid- or forefoot initial contact [27], [77], [79]. With regard to steppage gait, beyond lifting the legs higher, there are few differences in the gait profile to distinguish this from the other profiles [27], [77].

The current instrumented smart sock system could be improved leading to greater accuracy and the capacity to classify additional gait profiles. One option may be to include accelerometer data from a sensor close to the sacrum [45], which may assist when distinguishing gaits where hip movement is prominent such as is the case with diplegic and hemiplegic gaits. Another option to improve classification accuracy would potentially be to incorporate other types of sensors into the smart socks such as inertial measurement units (IMUs). The addition of data from multiple modalities

has been demonstrated to enable greater gait classification accuracy [42]. The challenge associated with this would be the incorporation of such a sensor into the sock with minimal impact on the sock profile and the user’s comfort experience.

One strength of this work is that the Bi-LSTM network was able to correctly classify the majority of the gait profiles for participants that were not part of the training data. This suggests that data overfitting was not a significant problem for the network and that the network generally used appropriate elements of the available data to make its classifications. It can, therefore, be suggested that the training dataset used was sufficient to limit overfitting and ensure the generalizability of the data during testing [83]. Based on this principle, it should be possible to use the current smart socks and Bi-LSTM network to collect data from clinical populations in order to test the capacity of the network to classify differences in gait between individuals with medical impairments that have led to their altered gait profiles.

IV. CONCLUSION

The instrumented smart sock presented in this article combined with a Bi-LSTM was capable of classifying five of seven different gait profiles. The deep-learning architectures used to interpret the data were revealed to be accurate, capable of distinguishing between different gait profiles, and robust enough to cope with data from different participants. Furthermore, this work indicates that the incorporation of three accelerometers has a significant advantage when compared to measuring the acceleration from a single point on the foot. In addition, the results suggest that if only one accelerometer is used, it should be positioned at the ankle rather than the toe or heel. This work has demonstrated a proof of concept and shows that different movement patterns can be identified by a trained Bi-LSTM using simple unprocessed accelerometry data and minimal interpretation by a clinician/researcher. The next step in the process of developing a product that could be used to assist in gait rehabilitation and real-time gait monitoring is to collect data from clinical populations who may present subtle differences in their movement profiles that cannot be replicated by able-bodied individuals.

APPENDIX

See Table III and Fig. 4.

(a)		Convolution Neural Network							
Output Class	Diplegic Gait	0	13	667	221	0	0	36	0.0%
		0.0%	0.2%	10.2%	3.4%	0.0%	0.0%	0.5%	100%
	Hemiplegic Gait	0	12	710	205	0	0	11	1.3%
		0.0%	0.2%	10.8%	3.1%	0.0%	0.0%	0.2%	98.7%
	Steppage Gait	0	32	552	348	0	0	5	58.9%
		0.0%	0.5%	8.4%	5.3%	0.0%	0.0%	0.1%	41.1%
	Normal Gait	0	49	546	327	0	0	16	34.9%
		0.0%	0.7%	8.3%	5.0%	0.0%	0.0%	0.2%	65.1%
Shuffling Gait	0	105	793	39	0	0	0	0.0%	
	0.0%	1.6%	12.1%	0.6%	0.0%	0.0%	0.0%	100%	
Foot Slap Gait	0	68	564	289	0	0	17	0.0%	
	0.0%	1.0%	8.6%	4.4%	0.0%	0.0%	0.3%	100%	
Stomping Gait	0	46	599	158	0	0	134	14.3%	
	0.0%	0.7%	9.1%	2.4%	0.0%	0.0%	2.0%	85.7%	
		NaN%	3.7%	12.5%	20.6%	NaN%	NaN%	61.2%	15.6%
		NaN%	96.3%	87.5%	79.4%	NaN%	NaN%	38.8%	84.4%
		Diplegic Gait	Hemiplegic Gait	Steppage Gait	Normal Gait	Shuffling Gait	Foot Slap Gait	Stomping Gait	
		Target Class							
(b)		BiLSTM-Convolution Neural Network							
Output Class	Diplegic Gait	624	0	0	0	113	200	0	66.6%
		9.5%	0.0%	0.0%	0.0%	1.7%	3.0%	0.0%	33.4%
	Hemiplegic Gait	0	607	0	331	0	0	0	64.7%
		0.0%	9.3%	0.0%	5.0%	0.0%	0.0%	0.0%	35.3%
	Steppage Gait	0	0	0	315	0	0	622	0.0%
		0.0%	0.0%	0.0%	4.8%	0.0%	0.0%	9.5%	100%
	Normal Gait	0	133	0	624	0	0	181	66.5%
		0.0%	2.0%	0.0%	9.5%	0.0%	0.0%	2.8%	33.5%
Shuffling Gait	0	302	6	0	617	12	0	65.8%	
	0.0%	4.6%	0.1%	0.0%	9.4%	0.2%	0.0%	34.2%	
Foot Slap Gait	212	0	0	0	4	95	627	10.1%	
	3.2%	0.0%	0.0%	0.0%	0.1%	1.4%	9.6%	89.9%	
Stomping Gait	0	0	0	0	0	0	937	100%	
	0.0%	0.0%	0.0%	0.0%	0.0%	0.0%	14.3%	0.0%	
		74.6%	58.3%	0.0%	49.1%	84.1%	30.9%	39.6%	53.4%
		25.4%	41.7%	100%	50.9%	15.9%	69.1%	60.4%	46.6%
		Diplegic Gait	Hemiplegic Gait	Steppage Gait	Normal Gait	Shuffling Gait	Foot Slap Gait	Stomping Gait	
		Target Class							
(c)		LSTM Neural Network							
Output Class	Diplegic Gait	624	0	14	0	0	0	0	97.8%
		9.5%	0.0%	0.2%	0.0%	0.0%	0.0%	0.0%	2.2%
	Hemiplegic Gait	7	190	0	71	3	0	0	70.1%
		0.1%	2.9%	0.0%	1.1%	0.0%	0.0%	0.0%	29.9%
	Steppage Gait	0	0	0	0	0	0	0	NaN%
		0.0%	0.0%	0.0%	0.0%	0.0%	0.0%	0.0%	NaN%
	Normal Gait	0	748	608	770	0	175	0	33.5%
		0.0%	11.4%	9.3%	11.7%	0.0%	2.7%	0.0%	66.5%
Shuffling Gait	277	0	0	3	934	0	0	76.9%	
	4.2%	0.0%	0.0%	0.0%	14.2%	0.0%	0.0%	23.1%	
Foot Slap Gait	0	0	0	10	0	0	0	0.0%	
	0.0%	0.0%	0.0%	0.2%	0.0%	0.0%	0.0%	100%	
Stomping Gait	29	0	315	84	0	763	937	44.0%	
	0.4%	0.0%	4.8%	1.3%	0.0%	11.6%	14.3%	56.0%	
		66.6%	20.3%	0.0%	82.1%	99.7%	0.0%	100%	52.7%
		33.4%	79.7%	100%	17.9%	0.3%	100%	0.0%	47.3%
		Diplegic Gait	Hemiplegic Gait	Steppage Gait	Normal Gait	Shuffling Gait	Foot Slap Gait	Stomping Gait	
		Target Class							
(d)		Support-Vector Machine (SVM) Network							
Output Class	Diplegic Gait	0	0	0	0	0	0	0	NaN%
		0.0%	0.0%	0.0%	0.0%	0.0%	0.0%	0.0%	NaN%
	Hemiplegic Gait	562	563	562	563	562	563	562	14.3%
		8.6%	8.6%	8.6%	8.6%	8.6%	8.6%	8.6%	85.7%
	Steppage Gait	0	0	0	0	0	0	0	NaN%
		0.0%	0.0%	0.0%	0.0%	0.0%	0.0%	0.0%	NaN%
	Normal Gait	375	375	375	375	375	375	375	14.3%
		5.7%	5.7%	5.7%	5.7%	5.7%	5.7%	5.7%	85.7%
Shuffling Gait	0	0	0	0	0	0	0	NaN%	
	0.0%	0.0%	0.0%	0.0%	0.0%	0.0%	0.0%	NaN%	
Foot Slap Gait	0	0	0	0	0	0	0	NaN%	
	0.0%	0.0%	0.0%	0.0%	0.0%	0.0%	0.0%	NaN%	
Stomping Gait	0	0	0	0	0	0	0	NaN%	
	0.0%	0.0%	0.0%	0.0%	0.0%	0.0%	0.0%	NaN%	
		0.0%	60.0%	0.0%	40.0%	0.0%	0.0%	0.0%	14.3%
		100%	40.0%	100%	60.0%	100%	100%	100%	85.7%
		Diplegic Gait	Hemiplegic Gait	Steppage Gait	Normal Gait	Shuffling Gait	Foot Slap Gait	Stomping Gait	
		Target Class							

Fig. 4. Results from the confusion matrices when classifying the various gait types utilizing three neural networks and an SVM classifier. Data captured by all three accelerometers from each sock was used for the classification. (a) Convolution neural network (overall accuracy 15.6%). (b) Bi-LSTM-convolution neural network (overall accuracy 53.4%). (c) LSTM neural network (overall accuracy 52.7%). (d) Support vector network (overall accuracy 14.3%).

ACKNOWLEDGMENT

Zahra Rahemtulla contributed to the development and implementation of the accelerometer yarns for motion detection. Kalana Marasinghe designed the graphical abstract of this article.

REFERENCES

- [1] A. Libanori, G. Chen, X. Zhao, Y. Zhou, and J. Chen, "Smart textiles for personalized healthcare," *Nature Electron.*, vol. 5, no. 3, pp. 142–156, Mar. 2022, doi: [10.1038/s41928-022-00723-z](https://doi.org/10.1038/s41928-022-00723-z).
- [2] H. W. Choi et al., "Smart textile lighting/display system with multi-functional fibre devices for large scale smart home and IoT applications," *Nature Commun.*, vol. 13, no. 1, Feb. 2022, Art. no. 814, doi: [10.1038/s41467-022-28459-6](https://doi.org/10.1038/s41467-022-28459-6).
- [3] J. Shi et al., "Smart textile-integrated microelectronic systems for wearable applications," *Adv. Mater.*, vol. 32, no. 5, Jul. 2019, Art. no. 1901958, doi: [10.1002/adma.201901958](https://doi.org/10.1002/adma.201901958).
- [4] C. Zhu et al., "A nature-inspired, flexible substrate strategy for future wearable electronics," *Small*, vol. 15, no. 35, Jun. 2019, Art. no. 1902440, doi: [10.1002/smll.201902440](https://doi.org/10.1002/smll.201902440).
- [5] M. Lin et al., "A high-performance, sensitive, wearable multifunctional sensor based on rubber/CNT for human motion and skin temperature detection," *Adv. Mater.*, vol. 34, no. 1, Oct. 2021, Art. no. 2107309, doi: [10.1002/adma.202107309](https://doi.org/10.1002/adma.202107309).
- [6] M. Bariya, H. Y. Y. Nyein, and A. Javey, "Wearable sweat sensors," *Nature Electron.*, vol. 1, no. 3, pp. 160–171, Mar. 2018, doi: [10.1038/s41928-018-0043-y](https://doi.org/10.1038/s41928-018-0043-y).
- [7] M. Umair, N. Chalabianloo, C. Sas, and C. Ersoy, "HRV and stress: A mixed-methods approach for comparison of wearable heart rate sensors for biofeedback," *IEEE Access*, vol. 9, pp. 14005–14024, 2021, doi: [10.1109/ACCESS.2021.3052131](https://doi.org/10.1109/ACCESS.2021.3052131).
- [8] K. Zhou, K. Dai, C. Liu, and C. Shen, "Flexible conductive polymer composites for smart wearable strain sensors," *SmartMat*, vol. 1, no. 1, Nov. 2020, Art. no. e1010, doi: [10.1002/smm2.1010](https://doi.org/10.1002/smm2.1010).
- [9] T. Yamada et al., "A stretchable carbon nanotube strain sensor for human-motion detection," *Nature Nanotechnol.*, vol. 6, no. 5, pp. 296–301, Mar. 2011, doi: [10.1038/nnano.2011.36](https://doi.org/10.1038/nnano.2011.36).
- [10] B. Bozali, J. J. F. van Dam, L. Plaude, and K. M. B. Jansen, "Development of hysteresis-free and linear knitted strain sensors for smart textile applications," in *Proc. IEEE Sensors*, Oct. 2021, pp. 1–4, doi: [10.1109/SENSOR47087.2021.9639613](https://doi.org/10.1109/SENSOR47087.2021.9639613).

- [11] I. H. López-Nava and A. Muñoz-Meléndez, "Wearable inertial sensors for human motion analysis: A review," *IEEE Sensors J.*, vol. 16, no. 22, pp. 7821–7834, Nov. 2016, doi: [10.1109/JSEN.2016.2609392](https://doi.org/10.1109/JSEN.2016.2609392).
- [12] P. Lugoda et al., "Coco stretch: Strain sensors based on natural coconut oil and carbon black filled elastomers," *Adv. Mater. Technol.*, vol. 6, no. 2, Dec. 2020, Art. no. 2000780, doi: [10.1002/admt.202000780](https://doi.org/10.1002/admt.202000780).
- [13] H. Schmidt, C. Werner, R. Bernhardt, S. Hesse, and J. Krüger, "Gait rehabilitation machines based on programmable footplates," *J. Neuro-Eng. Rehabil.*, vol. 4, no. 1, pp. 1–7, Feb. 2007, doi: [10.1186/1743-0003-4-2](https://doi.org/10.1186/1743-0003-4-2).
- [14] J. Muckell, Y. Young, and M. Leventhal, "A wearable motion tracking system to reduce direct care worker injuries," in *Proc. Int. Conf. Digit. Health*, Jul. 2017, pp. 202–206, doi: [10.1145/3079452.3079493](https://doi.org/10.1145/3079452.3079493).
- [15] A. K. Yetisen, J. L. Martínez-Hurtado, B. Únal, A. Khademhosseini, and H. Butt, "Wearables in medicine," *Adv. Mater.*, vol. 30, no. 33, Jun. 2018, Art. no. 1706910, doi: [10.1002/adma.201706910](https://doi.org/10.1002/adma.201706910).
- [16] S. D. Din et al., "Gait analysis with wearables predicts conversion to Parkinson disease," *Ann. Neurol.*, vol. 86, no. 3, pp. 357–367, Jul. 2019, doi: [10.1002/ana.25548](https://doi.org/10.1002/ana.25548).
- [17] L. N. Awad et al., "A soft robotic exosuit improves walking in patients after stroke," *Sci. Transl. Med.*, vol. 9, no. 400, Jul. 2017, Art. no. eaai9084, doi: [10.1126/scitranslmed.aai9084](https://doi.org/10.1126/scitranslmed.aai9084).
- [18] S. Armand, F. Moissenet, G. de Coulon, and A. Bonnefoy-Mazure, "Identifying and understanding gait deviations: Critical review and perspectives," *Movement Sport Sci., Sci. Motricité*, no. 98, pp. 77–88, 2017, doi: [10.1051/sm/2017016](https://doi.org/10.1051/sm/2017016).
- [19] N. Veronese et al., "Association between gait speed with mortality, cardiovascular disease and cancer: A systematic review and meta-analysis of prospective cohort studies," *J. Amer. Med. Directors Assoc.*, vol. 19, no. 11, pp. 981–988, Nov. 2018, doi: [10.1016/j.jamda.2018.06.007](https://doi.org/10.1016/j.jamda.2018.06.007).
- [20] S. Porta, A. Martínez, N. Millor, M. Gómez, and M. Izquierdo, "Relevance of sex, age and gait kinematics when predicting fall-risk and mortality in older adults," *J. Biomech.*, vol. 105, May 2020, Art. no. 109723, doi: [10.1016/j.jbiomech.2020.109723](https://doi.org/10.1016/j.jbiomech.2020.109723).
- [21] R. Verma, K. N. Arya, P. Sharma, and R. K. Garg, "Understanding gait control in post-stroke: Implications for management," *J. Bodywork Movement Therapies*, vol. 16, no. 1, pp. 14–21, Jan. 2012, doi: [10.1016/j.jbmt.2010.12.005](https://doi.org/10.1016/j.jbmt.2010.12.005).
- [22] N. Lefebvre, M. Degelaen, C. Truyers, I. Safin, and D. Beckwee, "Validity and reproducibility of inertial physilog sensors for spatiotemporal gait analysis in patients with stroke," *IEEE Trans. Neural Syst. Rehabil. Eng.*, vol. 27, no. 9, pp. 1865–1874, Sep. 2019, doi: [10.1109/TNSRE.2019.2930751](https://doi.org/10.1109/TNSRE.2019.2930751).
- [23] B. J. Lee, N.-Y. Joo, S. H. Kim, C. R. Kim, D. Yang, and D. Park, "Evaluation of balance functions using temporo-spatial gait analysis parameters in patients with brain lesions," *Sci. Rep.*, vol. 11, no. 1, pp. 1–7, Feb. 2021, doi: [10.1038/s41598-021-82358-2](https://doi.org/10.1038/s41598-021-82358-2).
- [24] M. Amboni et al., "Gait analysis may distinguish progressive supranuclear palsy and Parkinson disease since the earliest stages," *Sci. Rep.*, vol. 11, no. 1, pp. 1–9, Apr. 2021, doi: [10.1038/s41598-021-88877-2](https://doi.org/10.1038/s41598-021-88877-2).
- [25] P. D. Blasiis et al., "Short and long term effects of nabiximols on balance and walking assessed by 3D-gait analysis in people with multiple sclerosis and spasticity," *Multiple Sclerosis Rel. Disorders*, vol. 51, Jun. 2021, Art. no. 102805, doi: [10.1016/j.msard.2021.102805](https://doi.org/10.1016/j.msard.2021.102805).
- [26] S. Potluri, S. Ravuri, C. Diedrich, and L. Schega, "Deep learning based gait abnormality detection using wearable sensor system," in *Proc. 41st Annu. Int. Conf. IEEE Eng. Med. Biol. Soc. (EMBC)*, Jul. 2019, pp. 3613–3619, doi: [10.1109/EMBC.2019.8856454](https://doi.org/10.1109/EMBC.2019.8856454).
- [27] J. M. Baker, "Gait disorders," *Amer. J. Med.*, vol. 131, no. 6, pp. 602–607, Jun. 2018, doi: [10.1016/j.amjmed.2017.11.051](https://doi.org/10.1016/j.amjmed.2017.11.051).
- [28] W. Pirker and R. Katzenschlager, "Gait disorders in adults and the elderly," *Wiener Klinische Wochenschrift*, vol. 129, nos. 3–4, pp. 81–95, Oct. 2016, doi: [10.1007/s00508-016-1096-4](https://doi.org/10.1007/s00508-016-1096-4).
- [29] J. Nonnekes and A. Nieuwboer, "Towards personalized rehabilitation for gait impairments in Parkinson's disease," *J. Parkinson's Disease*, vol. 8, no. 1, pp. S101–S106, Dec. 2018, doi: [10.3233/jpd-181464](https://doi.org/10.3233/jpd-181464).
- [30] Y. Hutabarat, D. Owaki, and M. Hayashibe, "Recent advances in quantitative gait analysis using wearable sensors: A review," *IEEE Sensors J.*, vol. 21, no. 23, pp. 26470–26487, Dec. 2021, doi: [10.1109/JSEN.2021.3119658](https://doi.org/10.1109/JSEN.2021.3119658).
- [31] F. L. Buczek, M. J. Rainbow, K. M. Cooney, M. R. Walker, and J. O. Sanders, "Implications of using hierarchical and six degree-of-freedom models for normal gait analyses," *Gait Posture*, vol. 31, no. 1, pp. 57–63, Jan. 2010, doi: [10.1016/j.gaitpost.2009.08.245](https://doi.org/10.1016/j.gaitpost.2009.08.245).
- [32] X. Gu, F. Deligianni, B. Lo, W. Chen, and G. Yang, "Markerless gait analysis based on a single RGB camera," in *Proc. IEEE 15th Int. Conf. Wearable Implantable Body Sensor Netw. (BSN)*, Mar. 2018, pp. 42–45, doi: [10.1109/BSN.2018.8329654](https://doi.org/10.1109/BSN.2018.8329654).
- [33] D. Guffanti, A. Brunete, and M. Hernando, "Non-invasive multi-camera gait analysis system and its application to gender classification," *IEEE Access*, vol. 8, pp. 95734–95746, 2020, doi: [10.1109/ACCESS.2020.2995474](https://doi.org/10.1109/ACCESS.2020.2995474).
- [34] J. A. Albert, V. Owolabi, A. Gebel, C. M. Brahms, U. Granacher, and B. Arnrich, "Evaluation of the pose tracking performance of the azure Kinect and Kinect v2 for gait analysis in comparison with a gold standard: A pilot study," *Sensors*, vol. 20, no. 18, p. 5104, Sep. 2020, doi: [10.3390/s20185104](https://doi.org/10.3390/s20185104).
- [35] P. Fernández-González, A. Koutsou, A. Cuesta-Gómez, M. Carratalá-Tejada, J. C. Miangolarra-Page, and F. Molina-Rueda, "Reliability of Kinovea software and agreement with a three-dimensional motion system for gait analysis in healthy subjects," *Sensors*, vol. 20, no. 11, p. 3154, Jun. 2020, doi: [10.3390/s20113154](https://doi.org/10.3390/s20113154).
- [36] L. Simoni, A. Scarton, C. Macchi, F. Gori, G. Pasquini, and S. Pogliaghi, "Quantitative and qualitative running gait analysis through an innovative video-based approach," *Sensors*, vol. 21, no. 9, p. 2977, Apr. 2021, doi: [10.3390/s21092977](https://doi.org/10.3390/s21092977).
- [37] A. Murro-De-La-Herran, B. Garcia-Zapirain, and A. Mendez-Zorrilla, "Gait analysis methods: An overview of wearable and non-wearable systems, highlighting clinical applications," *Sensors*, vol. 14, no. 2, pp. 3362–3394, Feb. 2014, doi: [10.3390/s140203362](https://doi.org/10.3390/s140203362).
- [38] L. Middleton, A. A. Buss, A. Bazin, and M. S. Nixon, "A floor sensor system for gait recognition," in *Proc. 4th IEEE Workshop Autom. Identificat. Adv. Technol. (AutoID)*, Oct. 2005, pp. 171–176, doi: [10.1109/AUTOID.2005.2](https://doi.org/10.1109/AUTOID.2005.2).
- [39] T. Egerton, P. Thingstad, and J. L. Helbostad, "Comparison of programs for determining temporal-spatial gait variables from instrumented walkway data: PKmas versus GAITRite," *BMC Res. Notes*, vol. 7, no. 1, pp. 1–7, Aug. 2014, doi: [10.1186/1756-0500-7-542](https://doi.org/10.1186/1756-0500-7-542).
- [40] S. C. Wearing, L. F. Reed, and S. R. Urry, "Agreement between temporal and spatial gait parameters from an instrumented walkway and treadmill system at matched walking speed," *Gait Posture*, vol. 38, no. 3, pp. 380–384, Jul. 2013, doi: [10.1016/j.gaitpost.2012.12.017](https://doi.org/10.1016/j.gaitpost.2012.12.017).
- [41] C. Fricke, J. Alizadeh, N. Zakhary, T. B. Woost, M. Bogdan, and J. Classen, "Evaluation of three machine learning algorithms for the automatic classification of EMG patterns in gait disorders," *Frontiers Neurol.*, vol. 12, May 2021, Art. no. 666458, doi: [10.3389/fneur.2021.666458](https://doi.org/10.3389/fneur.2021.666458).
- [42] A. S. Alharthi, S. U. Yunas, and K. B. Ozanyan, "Deep learning for monitoring of human gait: A review," *IEEE Sensors J.*, vol. 19, no. 21, pp. 9575–9591, Nov. 2019, doi: [10.1109/JSEN.2019.2928777](https://doi.org/10.1109/JSEN.2019.2928777).
- [43] V. V. Shah et al., "Laboratory versus daily life gait characteristics in patients with multiple sclerosis, Parkinson's disease, and matched controls," *J. NeuroEng. Rehabil.*, vol. 17, no. 1, Dec. 2020, Art. no. 159, doi: [10.1186/s12984-020-00781-4](https://doi.org/10.1186/s12984-020-00781-4).
- [44] J. Shi et al., "Smart textile-integrated microelectronic systems for wearable applications," *Adv. Mater.*, vol. 32, no. 5, Feb. 2020, Art. no. 1901958. [Online]. Available: <https://onlinelibrary.wiley.com/doi/abs/10.1002/adma.201901958>
- [45] A. Mansfield and G. M. Lyons, "The use of accelerometry to detect heel contact events for use as a sensor in FES assisted walking," *Med. Eng. Phys.*, vol. 25, no. 10, pp. 879–885, Dec. 2003, doi: [10.1016/s1350-4533\(03\)00116-4](https://doi.org/10.1016/s1350-4533(03)00116-4).
- [46] W. Tao, T. Liu, R. Zheng, and H. Feng, "Gait analysis using wearable sensors," *Sensors*, vol. 12, no. 12, pp. 2255–2283, Feb. 2012, doi: [10.3390/s120202255](https://doi.org/10.3390/s120202255).
- [47] J.-T. Zhang, A. C. Novak, B. Brouwer, and Q. Li, "Concurrent validation of Xsens MVN measurement of lower limb joint angular kinematics," *Physiol. Meas.*, vol. 34, no. 8, pp. N63–N69, Jul. 2013, doi: [10.1088/0967-3334/34/8/n63](https://doi.org/10.1088/0967-3334/34/8/n63).
- [48] A. G. Leal-Junior, A. Frizzera, L. M. Avellar, C. Marques, and M. J. Pontes, "Polymer optical fiber for in-shoe monitoring of ground reaction forces during the gait," *IEEE Sensors J.*, vol. 18, no. 6, pp. 2362–2368, Mar. 2018, doi: [10.1109/JSEN.2018.2797363](https://doi.org/10.1109/JSEN.2018.2797363).
- [49] F. Lin, A. Wang, Y. Zhuang, M. R. Tomita, and W. Xu, "Smart insole: A wearable sensor device for unobtrusive gait monitoring in daily life," *IEEE Trans. Ind. Informat.*, vol. 12, no. 6, pp. 2281–2291, Dec. 2016, doi: [10.1109/TII.2016.2585643](https://doi.org/10.1109/TII.2016.2585643).
- [50] U. Sunarya et al., "Feature analysis of smart shoe sensors for classification of gait patterns," *Sensors*, vol. 20, no. 21, p. 6253, Nov. 2020, doi: [10.3390/s20216253](https://doi.org/10.3390/s20216253).

- [51] S. J. M. Bamberg, A. Y. Benbasat, D. M. Scarborough, D. E. Krebs, and J. A. Paradiso, "Gait analysis using a shoe-integrated wireless sensor system," *IEEE Trans. Inf. Technol. Biomed.*, vol. 12, no. 4, pp. 413–423, Jul. 2008, doi: [10.1109/TITB.2007.899493](https://doi.org/10.1109/TITB.2007.899493).
- [52] A. Turner and S. Hayes, "The classification of minor gait alterations using wearable sensors and deep learning," *IEEE Trans. Biomed. Eng.*, vol. 66, no. 11, pp. 3136–3145, Nov. 2019, doi: [10.1109/TBME.2019.2900863](https://doi.org/10.1109/TBME.2019.2900863).
- [53] O. Tirosh, R. Begg, E. Passmore, and N. Knopp-Steinberg, "Wearable textile sensor sock for gait analysis," in *Proc. 7th Int. Conf. Sens. Technol. (ICST)*, Dec. 2013, pp. 618–622, doi: [10.1109/icsent.2013.6727727](https://doi.org/10.1109/icsent.2013.6727727).
- [54] P. Eizentals, A. Katashev, and A. Oks, "Gait analysis by using smart socks system," *IOP Conf. Ser., Mater. Sci. Eng.*, vol. 459, Dec. 2018, Art. no. 012037, doi: [10.1088/1757-899x/459/1/012037](https://doi.org/10.1088/1757-899x/459/1/012037).
- [55] G. D'Addio et al., "Development of a prototype E-textile sock," in *Proc. 41st Annu. Int. Conf. IEEE Eng. Med. Biol. Soc. (EMBC)*, Jul. 2019, pp. 1749–1752, doi: [10.1109/EMBC.2019.8856739](https://doi.org/10.1109/EMBC.2019.8856739).
- [56] P. Eizentals, A. Katashev, A. Okss, Z. Pavare, and D. Balcuna, "Detection of excessive pronation and supination for walking and running gait with smart socks," in *Proc. World Congr. Med. Phys. Biomed. Eng. (IFMBE Proceedings)*. Singapore: Springer, May 2018, pp. 603–607, doi: [10.1007/978-981-10-9038-7_112](https://doi.org/10.1007/978-981-10-9038-7_112).
- [57] F. Amitrano, A. Coccia, L. Donisi, G. Pagano, G. Cesarelli, and G. D'Addio, "Gait analysis using wearable E-textile sock: An experimental study of test-retest reliability," in *Proc. IEEE Int. Symp. Med. Meas. Appl. (MeMeA)*, Jun. 2021, pp. 1–6, doi: [10.1109/MEMEA52024.2021.9478702](https://doi.org/10.1109/MEMEA52024.2021.9478702).
- [58] N. Carbonaro et al., "Exploiting resistive matrix technology to build a stretchable sensorized sock for gait analysis in daily life," *Sensors*, vol. 22, no. 5, p. 1761, Feb. 2022, doi: [10.3390/s22051761](https://doi.org/10.3390/s22051761).
- [59] N. Carbonaro, L. Arcarisi, F. Di Rienzo, A. Virdis, C. Vallati, and A. Tognetti, "A preliminary study on a new lightweight and flexible sensing sock for gait analysis," in *Proc. IEEE SENSORS*, Oct. 2020, pp. 1–4, doi: [10.1109/SENSORS47125.2020.9278682](https://doi.org/10.1109/SENSORS47125.2020.9278682).
- [60] M. Abtahi et al., "MagicSoc: An E-textile IoT system to quantify gait abnormalities," *Smart Health*, vols. 5–6, pp. 4–14, Jan. 2018, doi: [10.1016/j.smhl.2017.10.002](https://doi.org/10.1016/j.smhl.2017.10.002).
- [61] A. R. Anwar, H. Yu, and M. Vassallo, "Optimal foot location for placing wearable IMU sensors and automatic feature extraction for gait analysis," *IEEE Sensors J.*, vol. 18, no. 6, pp. 2555–2567, Mar. 2018, doi: [10.1109/JSEN.2017.2786587](https://doi.org/10.1109/JSEN.2017.2786587).
- [62] D. Jarchi, J. Pope, T. K. M. Lee, L. Tamjidi, A. Mirzaei, and S. Saneii, "A review on accelerometry-based gait analysis and emerging clinical applications," *IEEE Rev. Biomed. Eng.*, vol. 11, pp. 177–194, 2018, doi: [10.1109/RBME.2018.2807182](https://doi.org/10.1109/RBME.2018.2807182).
- [63] Z. Zhang et al., "Deep learning-enabled triboelectric smart socks for IoT-based gait analysis and VR applications," *NPJ Flexible Electron.*, vol. 4, no. 1, Oct. 2020, Art. no. 29, doi: [10.1038/s41528-020-00092-7](https://doi.org/10.1038/s41528-020-00092-7).
- [64] J. C. Costa, F. Spina, P. Lugoda, L. Garcia-Garcia, D. Roggen, and N. Münzenrieder, "Flexible sensors—From materials to applications," *Technologies*, vol. 7, no. 2, p. 35, Apr. 2019, doi: [10.3390/technologies7020035](https://doi.org/10.3390/technologies7020035).
- [65] A. M. Shahidi, T. Hughes-Riley, C. Oliveira, and T. Dias, "An investigation of the physical and electrical properties of knitted electrodes when subjected to multi-axial compression and abrasion," in *Proc. Int. Conf. Challenges, Opportunities, Innov. Appl. Electron. Textiles*, Jan. 2021, doi: [10.3390/proceedings2021068002](https://doi.org/10.3390/proceedings2021068002).
- [66] T. Hughes-Riley, C. Oliveira, R. Morris, and T. Dias, "The characterization of a pressure sensor constructed from a knitted spacer structure," *Digit. Med.*, vol. 5, no. 1, p. 22, 2019, doi: [10.4103/digm.digm_17_18](https://doi.org/10.4103/digm.digm_17_18).
- [67] G. Kim, C. C. Vu, and J. Kim, "Single-layer pressure textile sensors with woven conductive yarn circuit," *Appl. Sci.*, vol. 10, no. 8, p. 2877, Apr. 2020, doi: [10.3390/app10082877](https://doi.org/10.3390/app10082877).
- [68] K. Greff, R. K. Srivastava, J. Koutmik, B. R. Steunebrink, and J. Schmidhuber, "LSTM: A search space Odyssey," *IEEE Trans. Neural Netw. Learn. Syst.*, vol. 28, no. 10, pp. 2222–2232, Oct. 2017, doi: [10.1109/TNNLS.2016.2582924](https://doi.org/10.1109/TNNLS.2016.2582924).
- [69] M. Alotaibi and A. Mahmood, "Improved gait recognition based on specialized deep convolutional neural network," *Comput. Vis. Image Understand.*, vol. 164, pp. 103–110, Nov. 2017, doi: [10.1016/j.cviu.2017.10.004](https://doi.org/10.1016/j.cviu.2017.10.004).
- [70] C. F. Martindale, V. Christlein, P. Klumpp, and B. M. Eskofier, "Wearables-based multi-task gait and activity segmentation using recurrent neural networks," *Neurocomputing*, vol. 432, pp. 250–261, Apr. 2021, doi: [10.1016/j.neucom.2020.08.079](https://doi.org/10.1016/j.neucom.2020.08.079).
- [71] T. Hughes-Riley, P. Lugoda, T. Dias, C. Trabi, and R. Morris, "A study of thermistor performance within a textile structure," *Sensors*, vol. 17, no. 8, p. 1804, Aug. 2017, doi: [10.3390/s17081804](https://doi.org/10.3390/s17081804).
- [72] P. Lugoda, T. Hughes-Riley, R. Morris, and T. Dias, "A wearable textile thermograph," *Sensors*, vol. 18, no. 7, p. 2369, Jul. 2018, doi: [10.3390/s18072369](https://doi.org/10.3390/s18072369).
- [73] T. Hughes-Riley and T. Dias, "Developing an acoustic sensing yarn for health surveillance in a military setting," *Sensors*, vol. 18, no. 5, p. 1590, May 2018, doi: [10.3390/s18051590](https://doi.org/10.3390/s18051590).
- [74] A. Satharasinghe, T. Hughes-Riley, and T. Dias, "An investigation of a wash-durable solar energy harvesting textile," *Prog. Photovolt., Res. Appl.*, vol. 28, no. 6, pp. 578–592, Dec. 2019, doi: [10.1002/pip.3229](https://doi.org/10.1002/pip.3229).
- [75] Z. Rahemtulla, T. Hughes-Riley, and T. Dias, "Vibration-sensing electronic yarns for the monitoring of hand transmitted vibrations," *Sensors*, vol. 21, no. 8, p. 2780, Apr. 2021, doi: [10.3390/s21082780](https://doi.org/10.3390/s21082780).
- [76] S. M. Woolley, "Characteristics of gait in hemiplegia," *Topics Stroke Rehabil.*, vol. 7, no. 4, pp. 1–18, Jan. 2001, doi: [10.1310/jb16-v04f-jal5-h1uv](https://doi.org/10.1310/jb16-v04f-jal5-h1uv).
- [77] K. Shah, M. Solan, and E. Dawe, "The gait cycle and its variations with disease and injury," *Orthopaedics Trauma*, vol. 34, no. 3, pp. 153–160, Jun. 2020, doi: [10.1016/j.morth.2020.03.009](https://doi.org/10.1016/j.morth.2020.03.009).
- [78] R. G. Crowther, W. L. Spinks, A. S. Leicht, F. Quigley, and J. Golledge, "Relationship between temporal-spatial gait parameters, gait kinematics, walking performance, exercise capacity, and physical activity level in peripheral arterial disease," *J. Vascular Surg.*, vol. 45, no. 6, pp. 1172–1178, Jun. 2007, doi: [10.1016/j.jvs.2007.01.060](https://doi.org/10.1016/j.jvs.2007.01.060).
- [79] J. A. Blaya and H. Herr, "Adaptive control of a variable-impedance ankle-foot orthosis to assist drop-foot gait," *IEEE Trans. Neural Syst. Rehabil. Eng.*, vol. 12, no. 1, pp. 24–31, Mar. 2004, doi: [10.1109/TNSRE.2003.823266](https://doi.org/10.1109/TNSRE.2003.823266).
- [80] Y. Yu, X. Si, C. Hu, and Z. Jianxun, "A review of recurrent neural networks: LSTM cells and network architectures," *Neural Comput.*, vol. 31, no. 7, pp. 1235–1270, 2019.
- [81] H. Guo and Y. Sung, "Movement estimation using soft sensors based on bi-LSTM and two-layer LSTM for human motion capture," *Sensors*, vol. 20, no. 6, p. 1801, Mar. 2020.
- [82] S. Siami-Namini, N. Tavakoli, and A. S. Namin, "The performance of LSTM and BiLSTM in forecasting time series," in *Proc. IEEE Int. Conf. Big Data (Big Data)*, Dec. 2019, pp. 3285–3292.
- [83] S. Dai, L. Li, and Z. Li, "Modeling vehicle interactions via modified LSTM models for trajectory prediction," *IEEE Access*, vol. 7, pp. 38287–38296, 2019, doi: [10.1109/ACCESS.2019.2907000](https://doi.org/10.1109/ACCESS.2019.2907000).



Pasindu Lugoda (Fellow, IEEE) received the degree in electronic and communication engineering from the University of Nottingham Malaysia, Semenyih, Malaysia, in 2012, and the Ph.D. degree in electronic textiles from the Advanced Textiles Research Group (ATRG), Nottingham Trent University, Nottingham, U.K., in 2019.

He worked as a Textile Development Engineer with MAS Holdings from 2012 to 2014. Then, he was appointed as a Research Fellow with the Sensor Technology Research Centre, University of Sussex, Brighton, U.K., developing shape-sensing textiles for orthotic applications, from 2018 to 2020. He is also an Honorary Research Fellow with the University of Sussex. He is a Lecturer with the Department of Engineering, Nottingham Trent University. His main scientific interests are electronic textiles, wearable and flexible electronics, sensors, and medical devices.



Stephen Clive Hayes received the degree in sport science and the master's degree in sports biomechanics from Liverpool John Moores University, Liverpool, U.K., in 2005 and 2008, respectively, and the Ph.D. degree from the University of Hull, Hull, U.K., in 2020.

After several years in the industry, he returned to academia at the University of Hull, where he worked as a Specialist Biomechanics Laboratory Technician while undertaking his Ph.D. in sport science, investigating the use of technology in the rehabilitation of spinal cord injury. He has been appointed the role of Lecturer at the University of Hull in 2021. He is a Senior Lecturer in Sports Engineering with the Department of Engineering, Nottingham Trent University, Nottingham, U.K. His primary research interests are in gait analysis, movement quality, and injury rehabilitation.



Theodore Hughes-Riley received the degree in physics from Lancaster University, Lancaster, U.K., in 2009, and the Ph.D. degree from the University of Nottingham, Nottingham, U.K., in 2014.

He has worked at Nottingham Trent University, Nottingham, since 2013, initially as a Research Fellow with the Department of Physics and Mathematics, before moving to the Nottingham School of Art and Design in 2016 to develop electronic textiles. He is an Associate Professor in Electronic Textiles with the Nottingham School of Art and Design, Nottingham Trent University, and a member of the Advanced Textiles Research Group. His main research interests are electronic textiles, sensing systems, and medical devices.



Alexander Turner received the M.Sc. degree from the Department of Computer Science, University of York, York, U.K., and the Ph.D. degree from the Department of Electronic Engineering, University of York.

He is an Assistant Professor with the School of Computer Science, University of Nottingham, Nottingham, U.K., where he specializes in the application of machine learning to medical diagnostics and treatment. He joined the department in 2020 and before this, he was a Lecturer in Computer Science with the University of Hull, Hull, U.K., from 2016 to 2020, and a Postdoctoral Researcher with the Department of Electronic Engineering, University of York. In 2014, he was a Research Fellow with the Department of Clinical and Molecular Medicine, Norwegian University of Science and Technology (NTNU), Trondheim, Norway.



Mariana V. Martins is pursuing the M.Eng. degree in sports engineering with Nottingham Trent University, Nottingham, U.K.

Her main scientific interests are prosthetics, biomechanical performance, wearable and flexible electronics, and performance monitoring.



Ashley Cook is pursuing the M.Eng. degree in electronic engineering with Nottingham Trent University, Nottingham, U.K.

His interests lie in software infrastructure, circuit design, wearable textiles, and embedded systems.



Kaivalya Raval is pursuing the M.Eng. degree in sports engineering with Nottingham Trent University, Nottingham, U.K.

His key scientific research interests include biomechanical testing, motion tracking systems, smart textiles, sensors, and wearables for monitoring health and performance.



Carlos Oliveira is a Textile Technologist and a Knit CAD/CAM Programmer with over 25 years of experience ranging from sampling and production to liaising with garment technologists and designers. He is an Experimental Officer with the Advanced Textiles Research Group, Nottingham Trent University, Nottingham, U.K., and works on a variety of research and development projects. He has significant experience in using several types of computerized flat-bed knitting machines, yarn covering, knit-braid and braiding machines.

His main scientific interests are electronic textiles, smart textiles, and wearables.



Philip Breedon is a Professor of Smart Technologies at Nottingham Trent University, Nottingham, U.K. He is the NTU Lead for membership of the UK-Robotics and Autonomous Systems (UKRAS) network and is a member of the U.K.'s Department of Health National Institute for Health Research Invention for Innovation Funding Panel (NIHR i4i) and the Royal College of Surgeons MSK Robotic and Digital Surgery Subgroup. His research interests and latest projects center on new and emerging technologies and materials. This includes wearable technologies, 3-D/4-D printing, additive and subtractive manufacturing, rehabilitation technology, surgical robotics, cardiovascular devices, extended reality technologies and environments, and the surgical pathway and investigative research related to the utilization of "smart materials" for medical applications.

This includes wearable technologies, 3-D/4-D printing, additive and subtractive manufacturing, rehabilitation technology, surgical robotics, cardiovascular devices, extended reality technologies and environments, and the surgical pathway and investigative research related to the utilization of "smart materials" for medical applications.



Tilak Dias studied electrical and electronics engineering at the University of Moratuwa, Moratuwa, Sri Lanka, in 1969. He received the "Diplom-Ingenieur" degree in textile engineering from the Technische Universität in Dresden, Dresden, Germany, in 1981, and the "Dr.-Ingenieur" degree from the Universität Stuttgart, Stuttgart, Germany, in 1988.

He holds the Chair in Knitting at Nottingham Trent University, Nottingham, U.K. He has over 41 years of experience in knit structure design and knitting technology, and 20 years of experience developing electronic textiles.